Intensified liquid-liquid extraction of biomolecules using ionic liquids in small channels.

Yiota-Victoria Phakoukaki[1], Paul O'Shaughnessy[2], Panagiota Angeli[1*]

[1]ThAMeS Multiphase, Department of Chemical Engineering, UCL, Torrington Place, London WC1E 7JE

[2]Johnson Matthey Blounts Ct Rd, Sonning Common, Reading RG4 9NH

*Corresponding author: p.angeli@ucl.ac.uk

Abstract

The continuous extraction of an amino acid from an aqueous solution into an ionic liquid phase was studied experimentally in small channels, demonstrating a double intensification of the solvent used and overall process, respectively. Channels with 0.5, 1 and 2mm internal diameter were used for the extraction of the amino acid, L-tryptophan from an aqueous solution (0.005 mol.L^{-1}), into a hydrophobic ionic liquid, 1-Butyl-3-methylimidazolium Bis (trifluoromethanesulfonyl)imide, [C4mim][Tf$_2$N] in the presence of a crown ether extractant Dicyclohexano-18-crown-6, (DC18C6). A mechanism was proposed for the extraction which involved the ammonium centre of the amino acid forming hydrogen bonds with the 18-crown-6 part of the extractant at a 1:1 ratio. Partition coefficients up to 25 were obtained. The continuous extraction experiments were carried out during plug flow where the interfacial areas reported reached up to 5500 m^{2}m^{-3} at 50% volume fractions. Extraction efficiencies up to 90% were obtained for residence times less than 30 s. Overall mass transfer coefficients (K$_L$α), found reached up to 0.14 s^{-1}.

Nomenclature

A	Cross sectional area of capillaries [m^2]
B_o	Bond number = $\Delta\rho gD^2/\gamma$ [-]
C^*_{aq}	Equilibrium solute aqueous concentration [mol L^{-1}]
Ca	Capillary number = $\mu u_{mix}/\gamma$ [-]
$C_{aq}{}^*$	Aqueous equilibrium concentration of solute [mol L^{-1}]
$C_{aq,in}$	Aqueous phase initial concentration of solute [mol L^{-1}]
$C_{aq,out}$	Aqueous phase final concentration of solute [mol L^{-1}]
D	Internal diameter of channel [m]
E	Extraction efficiency [%]
g	Gravitational acceleration [m s^{-1}]
K	Dissociation constant [-]
K_L	Overall mass transfer coefficient [m^3 s^{-1}]
$K_L\alpha$	Overall volumetric mass transfer coefficient [s^{-1}]
L	Characteristic length [m]
P	Percentage extraction [%]
$P_{IL/W}$	Partition coefficient [-]
Q	Volumetric flow rate of fluid [m^3 s^{-1}]
Re	Reynold number [-]
SA	Surface area [m^2]
u	Mixture velocity [m s^{-1}]
V	Volume [m^3]
w	Width [m]
We	Weber number = $\rho u^2 D/\gamma$ [-]

Greek symbols

a	*Specific interfacial area* [m^2 m^{-3}]
γ	Surface tension [N m^{-1}]
δ	*Film thickness [mm]*
μ	*Dynamic viscosity* [kg m^{-1}s^{-1}]
ρ	*Density* [kg m^{-3}]
τ	*Residence time [s]*

Subscripts

aq	Aqueous phase
c	Continuous phase
ch	Channel

d	Dispersed phase
eff	Efficiency
IL	Ionic liquid
mix	Mixture
p	Plug
tot	Total
TU	Total cell

1. Introduction

Liquid-liquid solvent extraction remains one of the most attractive separation techniques due to its flexibility, simplicity, and effectiveness. The various current solvent and extractant combinations, as well as the discovery of new ones, depending on the application and desired separation efficiency, make solvent extraction a very versatile and powerful separation tool. Traditional equipment encountered in numerous industries include mixer-settlers, pulsed columns and centrifugal contactors [1]. However, despite the extensive use of solvent extraction in industry, conventional equipment can have many disadvantages that include large inventories, insufficient characterization and non-homogeneous mixing combined with long residence times. In the pharmaceuticals production specifically, the cost associated with downstream processing, purification and recovery of target biomolecules is one of the main issues that has limited the uptake of many products [2]. The development and testing of new biocompatible methods for the separation and purification of different bio-based products including amino acids, peptides, and proteins, is one of the most developing areas of biotechnology. Current bio-separation methods require several steps that are typically associated with both high energy and chemicals consumption. The overall cost of the separation and purification steps of the final bio-based products can reach up to 90% of the total manufacturing cost [3]. In liquid-liquid extractions, the solvent and extractant combinations should from a medical standpoint be as harmless as possible, significantly limiting the range of suitable solvents.

During the past two decades small scale and microfluidic devices have attracted significant attention as a means of intensifying processes. A large number of reviews have summarised their benefits in various fields ranging from rapid analysis and fine chemicals synthesis to reactions and separations [4]–[6]. Advantages of operating in small scales include increased mass transfer rates, minimisation of hazardous materials, improved control of hydrodynamics, reduced operating and capital costs due to the small size of equipment [7]–[9]. In addition, studies of two-phase liquid-liquid flows in micro-structured equipment including microchannels, micro/milli tubes and micro-packed beds, have shown regular and well-defined patterns, large interfacial areas and high mass transfer coefficients [10] .

On the pharmaceuticals industry in particular, small-scale equipment has predominantly been used in the drug discovery research and manipulation of biomolecules [11]–[13]. In their review, Mitic and Gernay summarised the ways process intensification has been applied to the manufacturing of small pharmaceutical molecules including micro reactors, ultrasound and

meso-scale tubular reactors [14] . Nonetheless, there is a clear gap in the literature for the extraction of biomolecules specifically in small-scale devices and consequently, the entire processes transition to continuous production.

Several authors have studied the hydrodynamic characteristics and flow patterns of two phase of flows in microchannels, as they affect the heat and mass transfer rates [14]–[18]. Despite the number of flow pattern maps published with either the continuous and dispersed phase velocities [19], [20], flow rates [21] or dimensionless numbers such as Weber (We) and Capillary (Ca) [22] as coordinates, the flow pattern transition boundaries are still difficult to predict and depend on the materials properties and geometrical features of the systems used. Plug (segmented or slug) flow is the most observed flow pattern in liquid-liquid systems and appears over a large range of flowrates [16], [23], [24]. In plug flow, the dispersed phase forms convex shape plugs that are separated from each other and from the channel wall by the continuous phase. The regime offers large interfacial areas, improved radial mixing due to circulation patterns in the two phases and reduced axial mixing, which enhance mass transfer and improve uniformity [8]. Recent reviews have summarised liquid-liquid extractions in microchannels [6], [8], [9], [25] .

In liquid-liquid extractions, volatile organic solvents are often used. Despite the economic advantages, the application of conventional organic solvents such as toluene, ethyl acetate or hexane is accompanied by major disadvantages including high volatility, toxicity and the possibility of denaturing the biomolecules such as proteins or enzymes. Therefore, there is a drive to replace the volatile organic solvents with new green extraction media. Recently, ionic liquids (ILs) or IL- based aqueous biphasic systems (ABS) have been proposed as alternatives [2]. Nonetheless, limited literature is available on the use of ionic liquids for two phase operations in small channels.

Ionic liquids are organic salts with low melting points, which are liquid at room temperature. They have unique properties including low vapour pressures, good thermal stability, high ion density and high ionic conductivity [26]. Moreover, from the pharmaceutical perspective, ILs are compatible solvents that do not inactivate biomolecules such as enzymes, thus ensuring their structural integrity [27]. Modification of both the cation and anion or mixing of the ILs with other liquids, enables fine tuning of their solvent properties making them ideal for specific separations [28]. In recent years, they have been considered in applications including liquid-liquid extraction of metal ions and organic compounds resulting in high partition coefficients

[10], [29]–[32]. Ionic liquids have demonstrated a clear capability of dissolving a wide variety of both organic and inorganic compounds, however, some disadvantages include large viscosities and high manufacturing costs [33]. Nonetheless, following the rapid advances, BASF demonstrated the first successful application of ionic liquids on commercial scale, the BASIL (Biphasic Acid Scavenging utilising Ionic Liquids) process, [34] followed by others [35].

A number of studies have explored the application of IL on the extraction of amino acids and other biomolecules from aqueous solutions with the review by Ventura et. al, summarizing the recent developments and advantages of IL in bioseparations [36]. High partition coefficients have been reported that are traditionally difficult to achieve with conventional organic solvents. The extraction from aqueous solutions has been performed both with and without the aid of different macrocylic ligands [27], [28], [31], [37]–[45]. In all these studies, however, equilibrium conditions in batch systems were considered. To the authors' knowledge, there are no studies available for the continuous extraction of biomolecules in small channels using ionic liquids.

In this work, a new combination of an IL with a macrocylic extractant is proposed for the separation of an amino acid (L-tryptophan) from aqueous solutions. Amino acids were selected as model molecules because their charged nature reproduces the behaviour of many other biomolecules. They also act as the main building blocks of more complicated molecules including peptides, enzymes and proteins. The extractions were carried, for the first time, continuously in small flow channels, providing a double process intensification which combines novel ionic liquids and enhanced mass transfer rates in intensified units. In what follows, the selection of the IL and the extractant are first discussed. The experimental set up and conditions are then described. Equilibrium experiments were carried out to find the mechanism of the extraction and the partition coefficients. The two-phase flow patterns in the small channels are then shown, to identify the conditions where plug flow occurs. The results on extraction and mass transfer coefficients are finally presented and discussed in relation to the hydrodynamic properties of plug flow and to conventional extraction equipment.

## 2. Ionic liquid selection for the separation of amino acids

Amino acids can exist in three different equilibrium forms in aqueous solutions: zwitterionic, anionic and cationic. At neutral pH the amino acids are in the zwitterionic form; as the pH is

increased with the addition of hydroxide ions to the solution, the hydrogen ion is removed from the -NH_3^+ group. Similarly, by decreasing the pH with the addition of an acid, the -COO^- part of the zwitterion picks up a hydrogen ion and becomes cationic. The two dissociation equilibria for amino acids in aqueous solutions are illustrated in Eq. (1) and (2) representing the amine protonation and the acid dissociation respectively.

$$H_2A^+ \overset{K_{AmH1}}{\Longleftrightarrow} H^+ + HA \tag{1}$$

$$HA \overset{K_{AmH2}}{\Longleftrightarrow} H^+ + A^- \tag{2}$$

where H_2A^+ HA, A^- are the cationic, zwitterionic, and anionic form of the amino acid, respectively, illustrated in Fig. 1.

The amino acid L-tryptophan was used as the model amino acid to be extracted from aqueous solutions. Its R side chain makes it a non-polar aromatic amino acid known to be able to form hydrogen bonds. It has been the model molecule for several ionic liquid extraction papers and was therefore selected for validation and comparison of results [28], [40], [41]. In aqueous solution the dissociation constants of L-tryptophan are $pK_1= 2.38$ and $pK_2= 9.38$. Similarly, Eq. (3) and (4) show the water and nitric acid dissociation respectively [40]. Nitric acid being a strong acid will always dissociate and the following equilibrium is therefore present.

$$H_2O \overset{K_{AH2O}}{\Longleftrightarrow} H^+ + OH^- \tag{3}$$

$$HNO_3 \overset{K_{AHNO3}}{\Longleftrightarrow} H^+ + NO_3^- \tag{4}$$
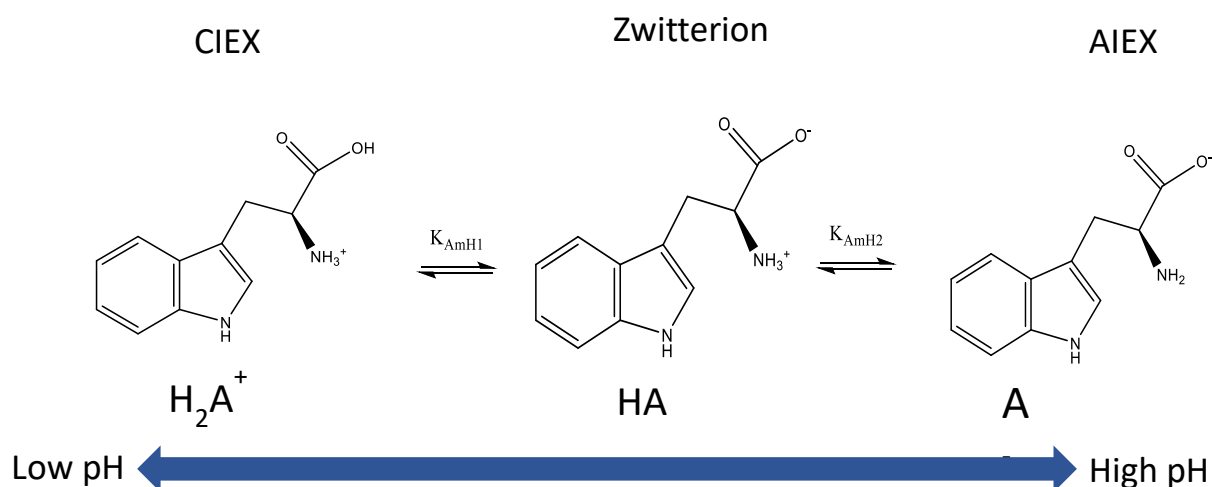
**Fig. 1.** Chemical structure of amino acid, L-tryptophan dissociation in aqueous solution.

Compared to traditional organic solvents in which amino acids have negligible solubility without the aid of extractants, certain families of ionic liquid have been reported to aid the extraction of amino acids without extractant. The anion of the ionic liquid, predominantly BF_4^- or PF_6^- binds to the cationic form of the amino acid through electrostatic forces [39], [40], [42], [45]. However, the BF_4^- anion is not stable in the presence of water for a range of pH and temperature values, while the PF_6^- anion has processing problems and can decompose to form hydrofluoric acid [46]. In the current studies, we selected the Tf_2N^- anion which is more stable and less toxic. This anion, however, has less concentrated charge, and a crown ether extractant was added to increase the partition coefficient. The crown ether with an 18-crown-6 was finally selected as it has shown high extraction of amino acids (92-96%) by forming a 1:1 complex [28], [47]. Furthermore, we used a short chain imidazolium IL cation, C_4mim, as it has low toxicity compared to longer chain ones. Moreover, the shorter chain allows for better electrostatic attractions of the amino acid with the IL anion. Imidazolium cations with longer alkyl chains are expected to disrupt the forces between the IL anion and the amino acid cation resulting in lower partition.

3. Experimental set-up and procedure

Amino-acid, L-tryptophan ($C_{11}H_{12}N_2O_2$) was purchased from Sigma-Aldrich, (UK) with a 98% purity and a molecular weight of 204.32 g/mol (CAS number: 73-22-3). The extractant, Dicyclohexano-18-crown-6 (DC18C6) was purchased as a mixture of stereoisomers at purity grade 98% crystalline solid form, from Fisher Scientific (UK) (CAS number: 16069-36-6). The ionic liquid, 1-Butyl-3-methylimidazolium Bis(trifluoromethanesulfonyl)imide, [C4mim] [T f_2 N] at 98 % purity grade was purchased from Sigma-Aldrich (UK) (CAS number: 174899-83-3). 70% concentrated nitric Acid (HNO_3) (Sigma-Aldrich, UK) was used to balance the pH of the aqueous solution. Fig. 2 illustrates the chemical structures of the crown ether extractant, the amino acid and the ionic liquid ions respectively.

The experiments were carried out at atmospheric pressure and room temperature (T= 298K). The pH was kept constant for all experiments (pH=1) and measured using a pen-type pH meter (Velleman) with a 0.2 pH accuracy. To determine the concentration of amino acid in the aqueous phase known concentrations of amino acid were prepared with an accuracy of 10^{-4} g and a calibration curve was produced. A double beam Cary-60 high- end UV-Vis spectrometer (Agilent UK) was used at 280 nm and 300nm wavelength to detect L-tryptophan and 1-Butyl-3-methylimidazolium, respectively.
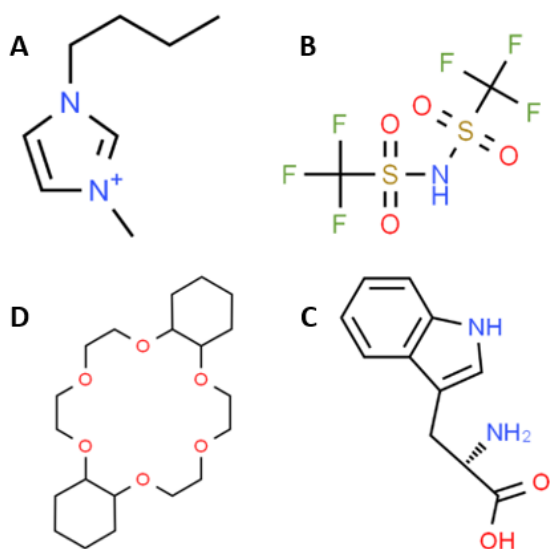
Fig. 2. Chemical structure A: Ionic liquid cation 1-Butyl-3-methylimidazolium, B: Ionic liquid anion Bis(trifluoromethanesulfonyl)imide C: Dicyclohexano-18-crown-6, D: L-tryptophan.

For the solvent extraction, the two immiscible phases were an aqueous solution of L-tryptophan and an ionic liquid/crown ether solution. For the equilibrium experiments a known amount of the amino-acid was dissolved in distilled water (concertation range 5×10^{-4}-2×10^{-3} mol L^{-1}) and a calibration curve was produced for different amino acid concentrations. The pH of the solution, unless otherwise stated, was adjusted with HNO$_3$ to maintain a constant pH=1 and to ensure the amino- acid is in its cationic form. 5mL of the aqueous solution was placed in stoppered vessels with an equal volume of the ionic liquid phase C$_4$mimTf$_2$N and mixed for 2 hours using a magnetic stirrer. The ionic liquid is hygroscopic, so it was pre-equilibrated by mixing it with the aqueous solution for 45 min prior to the extraction experiments. The viscosity of the ionic liquid before and after it was saturated with water was measured using a digital Rheometer DV-111 Ultra (Brookfield), illustrated in Table 1.The surface and interfacial tension were measured with the pendant drop method using a DSA100E drop shape analyser (KRÜSS Scientific). For the equilibrium experiments the concentration of the crown ether was varied from 5×10^{-4}-2×10^{-2} mol L^{-1} to determine its effect on the extraction mechanism. After equilibrium was achieved the two phases were separated and the partition coefficient P$_{IL/W}$ between the ionic liquid and the aqueous phases was calculated as follows.

$$P_{\frac{IL}{W}} = \frac{C_{aq,in} - C_{aq,fin}}{C_{aq,fin}} \qquad (5)$$

where C$_{aq,in}$ is the initial and C$_{aq,fin}$ was the final the amino acid concentration respectively in the aqueous phase.

Tab. 1: Physical properties of aqueous phase and ionic liquid C_4mimTf_2N before and after saturation with aqueous phase.

Physical properties	Pure IL	Water Saturated IL	Deionised Water
Viscosity, μ (kg m^{-1} s^{-1})	0.052	0.041	0.001
Density, ρ (kg m^{-3})	1420	1390	1000
Surface tension, σ (kg m$^{-3)}$)	31.3 x 10^{-3}	31.6 x 10^{-3}	73.10 x 10^{-3}
Interfacial tension,γ (N m^{-1})	12.3 x 10^{-3}		

The continuous flow extraction investigations in small channels were carried out in the set-up depicted in Fig 3. High precision continuous syringe pumps (Kd Scientific) were used to feed the two liquid phases separately in the main circular channel made of PTFE via a T-junction inlet configuration. The inlet was made of FEP and all sub-channels had the same internal diameters as that of the main test section. The ionic liquid phase was fed from the side channel at the same axis as the main one (see Fig. 3.) and was always the continuous phase in contact with the wall, while the aqueous phase was fed from the side channel as the dispersed phase (plug). The extraction experiments were performed in channels with three different internal diameters (0.5, 1 and 2 mm) while the lengths varied from 10-50cm. The flow in the main channel was visualised and flow patterns were recorded using a Photron Fatcam- ultima high speed camera at 2000- 4000Hz. The test section was illuminated with a 60W continuous arc lamp. To minimise reflections and improve the images, a visualization box filled with water, that matched the refractive index of the channel wall, was used to enclose the tube. A post processing routine was developed using MATLAB (MathWorks) to analyse the images obtained and detect the plug interface. A threshold pixel value was used to discriminate the dispersed and continuous phases in the images, while a lower threshold value was used to detect the channel wall. From the position of the plug relative to the channel wall its length and the film thickness were calculated. The values of plug length and film thickness where averaged over 10 images and the low values of standard deviation of up to 3% confirm the regularity of the plug flow pattern for mixture velocities in the range 0.01m/s to 0.05 m/s.

After the test section, the mixture of the two phases was separated in-line using a membrane-based flow separator (SEP-10 Zaiput Flow Technologies). The membrane used was made of PTFE (part number IL-900-S10) and is hydrophobic, thus allowing the ionic liquid phase to permeate it, while the aqueous passed over it. The maximum flow rates that the separator can effectively operate with no retention or breakthrough depend not only on the membrane used,

but also on the viscosity and interfacial tension of the two fluids. For the fluids used in this study, the maximum flow rate was approximately 3 m^3/s. All experiments were repeated at least three times. An error of the initial concentration of the amino acid in the aqueous phase was estimated (~2%).
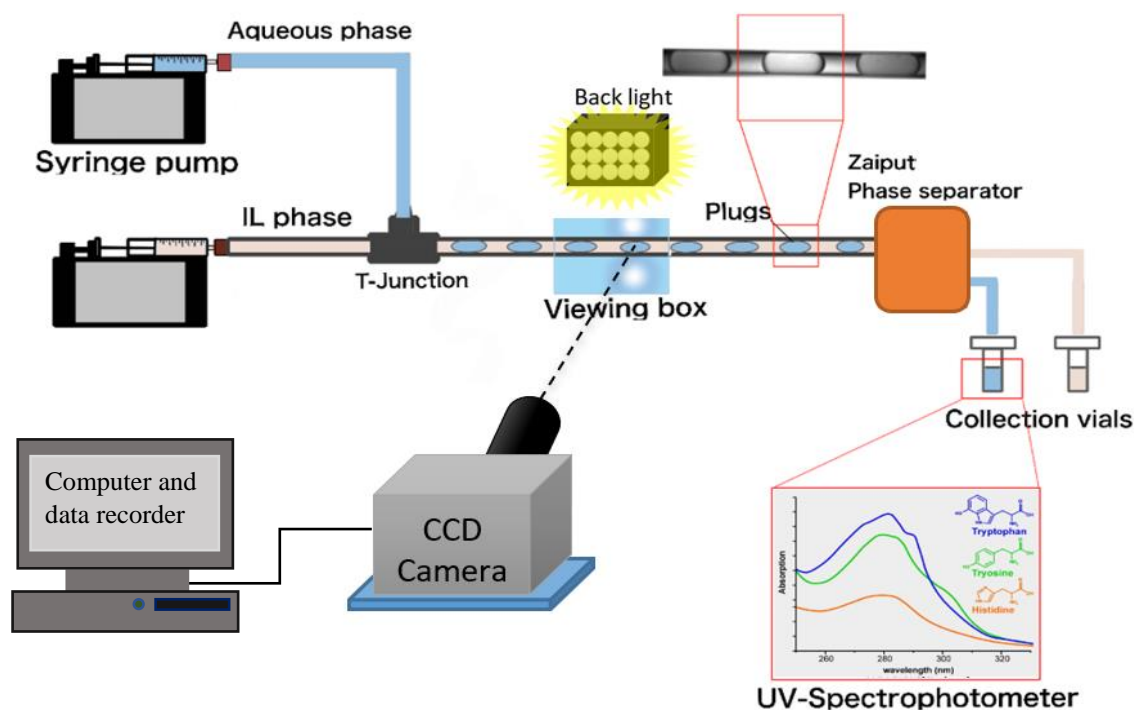
Fig. 3. Experimental set-up of liquid-liquid extraction in small channels for channel diameters 0.5, 1 and 2mm.

4. Mechanism of extraction

The amino acid extraction into the ionic liquid was performed with and without the aid of an extractant. Eq. (6) below is the ion- exchange equilibrium equation proposed for the extraction of an amino acid into an IL without the aid of an extractant. A similar mechanism was proposed by Absalan et.al, for imidazolium based ionic liquids with [BF$_4^-$] and [PF$_6^-$] anions [42].

$$[H_2A^+]_{(aq)+}[C_4mim^+][Tf_2N^-]_{(IL)} \Leftrightarrow [C_4mim^+]_{(aq)} + [H_2A^+][Tf_2N^-]_{(IL)} \qquad (6)$$
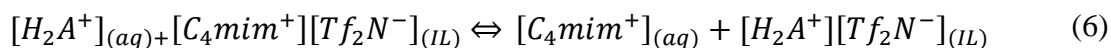
The extraction at pH> pK$_1$ was close to zero (where the amino acid is in the zwitterionic form), while partition coefficients in the range 0.9-1.6 were reported at pH < pK$_1$. This confirmed the above mechanism proposed involving the cationic amino acid and the anion of the IL and the presence of electrostatic interactions responsible for the extraction. As a result, for all the experiments in the microchannels the pH of the aqueous solution was kept at 1 to maximise the extraction of the cationic amino acid. The Tf_2N^- anion has a less dense negative charge than

the IL anions reported in the literature and gives low extraction. To increase the partition coefficient, a crown ether extractant was added.

The addition of crown ether (CE) allows for two different equilibrium equations (Eq. (7) and (8)), to describe the extraction, assuming electroneutrality. A similar mechanism with the same extract but different ionic liquids was proposed by Smirnova et.al [28]. Firstly, a cation exchange takes place involving the imidazolium cation of the ionic liquid and the pronated amino acid resulting in its partitioning into the aqueous phase shown in Eq. (7). The partitioning of the amino acid into the IL phase is assisted by the hydrogen bonding association of the cationic amino acid proton and the macrocyclic crown ether.

$$[H_2A^+]_{(aq)} + [CE]_{(IL)} + [C_4mim^+]_{(IL)} \Leftrightarrow [H_2A^+][CE]_{(IL)} + [C_4mim^+]_{(aq)} \qquad (7)$$
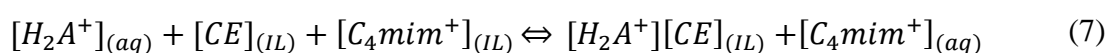
Secondly, the anion of the ionic liquid then forms a complex, acting as the counter-ion for the amino acid cation in the IL phase illustrated in Eq. (8).

$$[H_2A^+][CE]_{(IL)} + [Tf_2N^-]_{(IL)} \Leftrightarrow [H_2A^+][CE][Tf_2N^-]_{(IL)} \qquad (8)$$
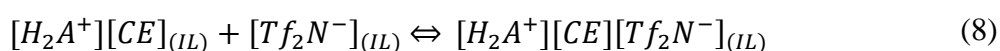
As opposed to extraction with conventional organic solvents a counter anion was not specifically introduced. Therefore, it could be expected that the counter-ion is the nitrate anion of the nitric acid added to balance the pH of the solution. However, the calculated partition coefficient obtained was not affected by increases the nitric acid concentrations. As a result, it is proposed that the ionic liquid anion is responsible for providing the counter-ion for the amino acid cations.

Moreover, after the extraction was performed UV analysis of the aqueous phase at equilibrium exhibited a peak at 300nm due to the 1-Butyl-3-methylimidazolium in the aqueous phase. It was found that increasing the initial amino acid concentration from 5×10^{-4} mol/L to 5×10^{-3} mol/L gave an increase in this absorbance at 300nm. This strongly supports the conclusion that an ion exchange mechanism is occurring for the extraction of L-tryptophan. The exact mechanism of this extraction will be the subject of future study.

It is expected that the H_3N^+ part of the amino acid binds to the 18-crown-6 using all six oxygens as donor atoms. The crown ether-amino acid complex formed on the aqueous-IL interface then moves into the ionic liquid. As a result, the amino acid to extractant ratio should be 1:1 [47]–[50]. To confirm this mechanism, equilibrium experiments were carried out as described above, where the amino acid concentration was kept constant (0.005,0.002,0.0005 mol/L) while the crown ether concentration was increased from 0.0005 to 0.05 mol/L (amino acid to extractant

concentration ratios from 1:1 to 1:10). As can be seen from Fig. 4 the slope of the curves, for $LogP_{IL/W}= f(LogCE)$ was approximately equal to 1 for all three amino acid concentrations tested. This confirms the mechanism proposed above involving the ammonium centre of the amino acid forming hydrogen bonds with the 18-crown-6 part of the crown ether.
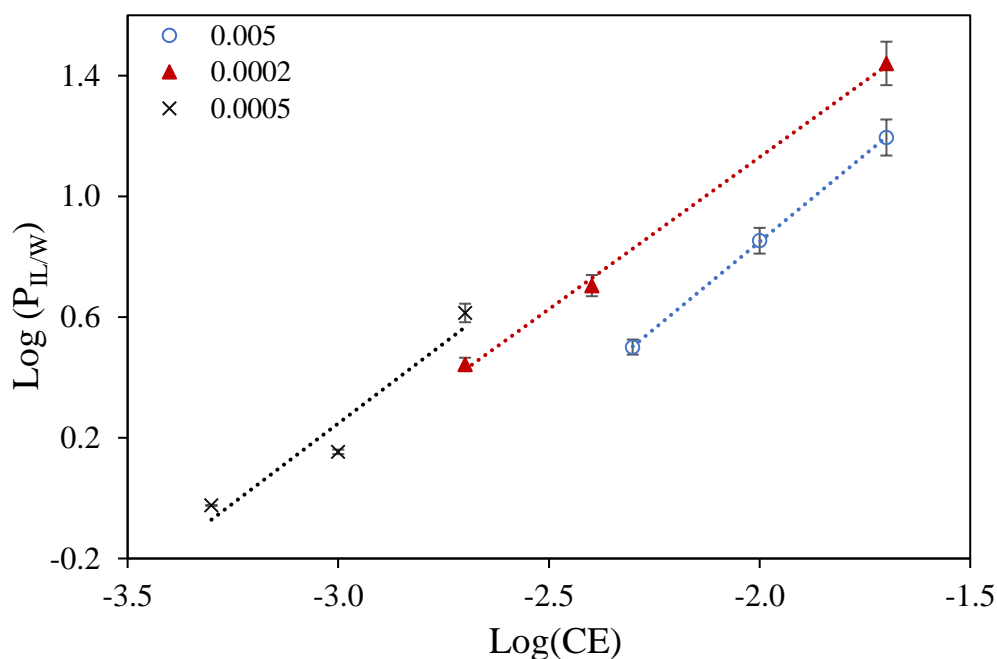
Fig. 4. Dependence of crown ether concentration on extraction of L-tryptophan (5 x10 $^{-4}$- 5 x 10^{-3} mol L^{-1}) into C_4mimTf_2N.
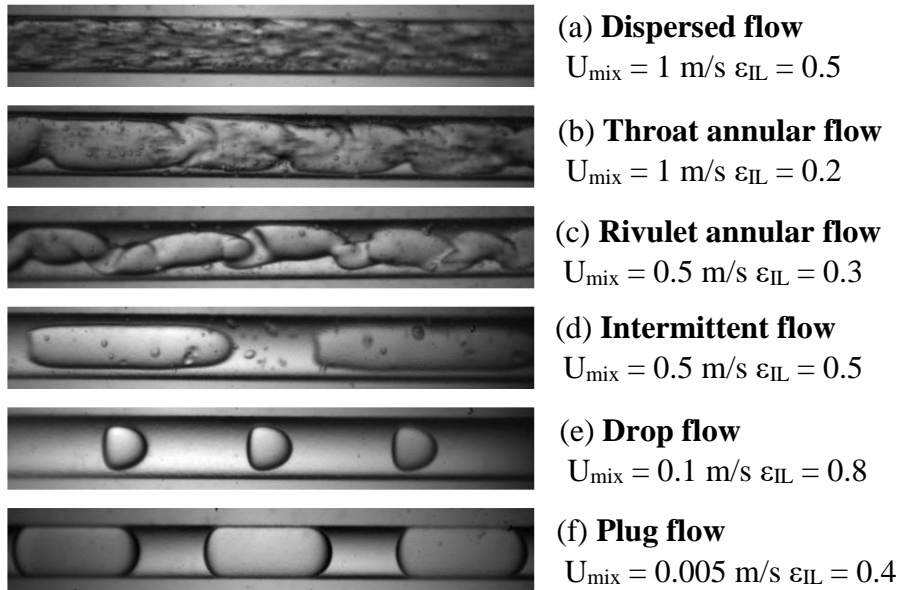
5. Flow patterns in small channels

In all experiments in the hydrophobic channels, the aqueous phase was dispersed, and the ionic liquid phase was continuous and separated the plugs form the channel wall. Ionic liquids are significantly more viscous than organic solvents that have previously been used in two-phase flows in small channels. Therefore, it is important to determine under what conditions, plug flow occurs. The flow patterns observed are presented in Fig. 5 for the 0.5 mm channel. These include plug, drop, dispersed and two different types of annular flow (throat and rivulet). The flow pattern maps were repeated with and without the addition of the extractant and amino acid. However, the differences between the patterns were insignificant, perhaps because of the low concentrations used.

The flow patterns for the 0.5 mm. channel are summarised in the map in Fig. 6 with the Capillary number (see Eq. (9)) and the ionic liquid volume fraction, $(\varepsilon_{IL}=Q_{IL}/Q_{mix})$ as coordinates.

$$Ca = \frac{\mu u_{mix}}{\sigma} \qquad (9)$$

The Capillary number (ratio of viscous over inertial forces) was chosen because the Bond number ($B_o = (\Delta \rho g D^2 / \sigma)$ was found to be 0.08, 0.34 and 1.34 for channel internal diameters 0.5, 1 and 2mm respectively, suggesting that interfacial forces dominate over gravitational ones [51]. In addition, the Reynolds numbers are less that one suggesting that viscous forces dominate the inertial ones. Plug flow (with the aqueous mixture as the dispersed phase plugs and the IL as the continuous phase) was dominant, at all ionic liquid volume fractions, at low mixture velocities when the interfacial forces responsible for stabilising the plug were dominant. As the effect of inertia increases with increasing mixture velocities and Ca, interfacial disturbances were observed in the plugs and the flow pattern changed to the intermittent regime. In this regime, also called plug and train flow (see Fig. 5 (d) and Fig.6), small droplets were observed, occasionally breaking up from the formed plugs, while larger droplets were noticed in the 2mm channel compared to the 0.5mm.


(a) **Dispersed flow**
$U_{mix} = 1$ m/s $\varepsilon_{IL} = 0.5$

(b) **Throat annular flow**
$U_{mix} = 1$ m/s $\varepsilon_{IL} = 0.2$

(c) **Rivulet annular flow**
$U_{mix} = 0.5$ m/s $\varepsilon_{IL} = 0.3$

(d) **Intermittent flow**
$U_{mix} = 0.5$ m/s $\varepsilon_{IL} = 0.5$

(e) **Drop flow**
$U_{mix} = 0.1$ m/s $\varepsilon_{IL} = 0.8$

(f) **Plug flow**
$U_{mix} = 0.005$ m/s $\varepsilon_{IL} = 0.4$

Fig. 5. Photographs of Ionic liquid [C4mim][Tf$_2$N]-water two-phase flow patterns in microchannels for various mixture velocities and phase volume factions.

As the Capillary number increases and at high IL volume fractions, plug flow transitions to regular drop flow due to the lower aqueous phase volume fraction in the channel. Dispersed flow appeared at high mixture velocities, $u_{mix} > 1$m/s for the 0.5 mm channel. At high mixture velocities and low IL volume fraction, the inertia of the aqueous phase is sufficient to break through the IL phase which is in contact with the wall and annular flow forms.
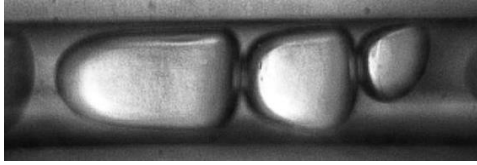
Fig. 6. Intermittent drop and train flow for 2mm channel, ionic liquid volume fraction 0.5, mixture Velocity 0.4 m/s.

When the channel diameter increased to 1mm and later 2mm, the boundary of the plug flow shifted to lower capillary numbers respectively, as shown in Fig. 7. At the larger 2mm channel, where interfacial forces are less prominent, the interfacial undulations during plug flow were more frequent and plugs and drops of different sizes were observed (see Fig. 5). The irregularity of the plug shapes in plug flow was confirmed by the deviation of the plug length. When comparing the 0.5 to the 2 mm channels, the standard deviation in the length of consecutive plugs was ~ 2% less for the small channel. Dispersed flows appeared at $u_{mix} > 0.06$ m/s for the 2mm internal diameter channel where inertial forces dominate. An indication of this is the Weber number (We= $\rho u^2 D/\sigma$ showing the dependence of mixture velocity, u_{mix} on the inertia forces. At Weber numbers less than 1 the interfacial forces responsible for stabilising the plugs are dominant. For channels with larger channel diameters, D this therefore happens at lower mixture velocities. Based on the map, the continuous extraction experiments in the small channels (section 6), were performed for mixture velocities (0.01-0.05 m/s) to ensure regular plug flow in all channel diameters tested.
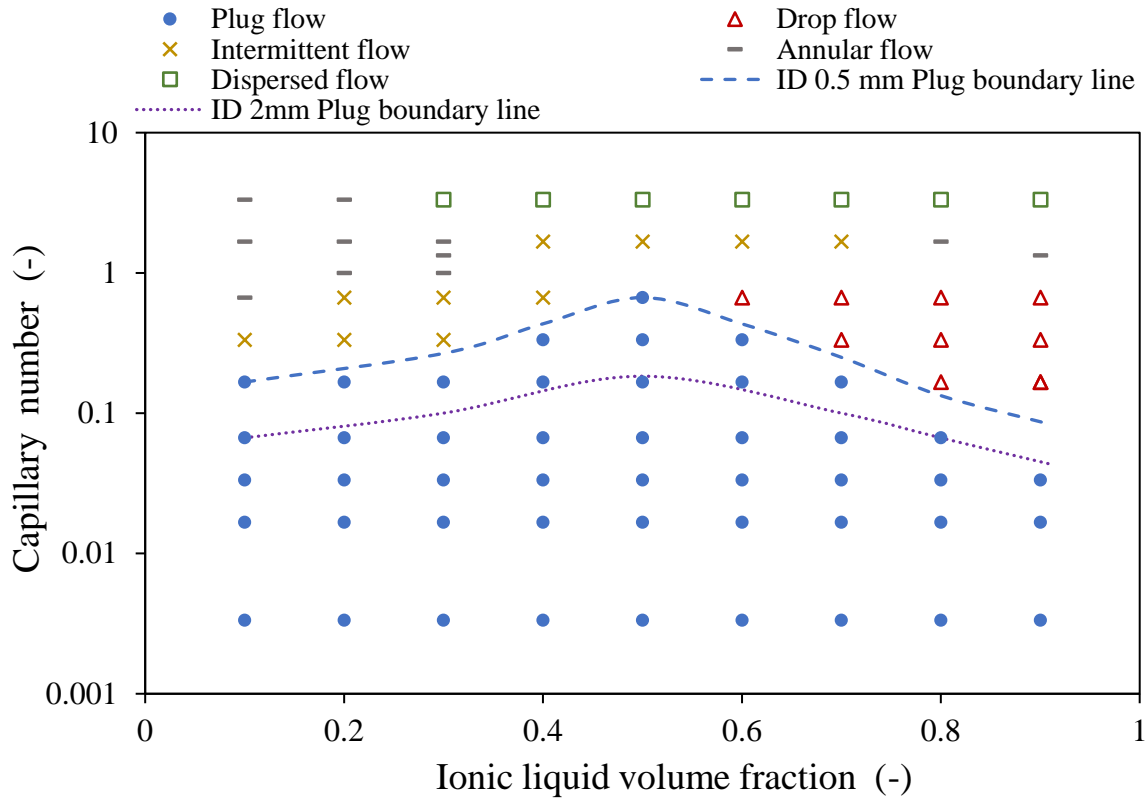
Fig. 7. Flow pattern map for aqueous ionic liquid phase [C4mim] [Tf$_2$N] in small channel with 0.5 mm internal diameter. Illustrates plug flow region for 0.5 and 2mm channel respectively.

5.1 Interfacial area for mass transfer in plug flow

From the images acquired, the plug length and film thickness at each channel diameter and at increasing mixture velocities were measured. It was found that when the mixture velocity increased, for equal volume fractions of the two phases, the length of the plugs decreased while their number increased, due to the increasingly rapid penetration of the dispersed phase into the continuous one at the inlet. Furthermore, the plug shape changed from a capsule with round ends to a bullet one, as illustrated in Fig. 8.
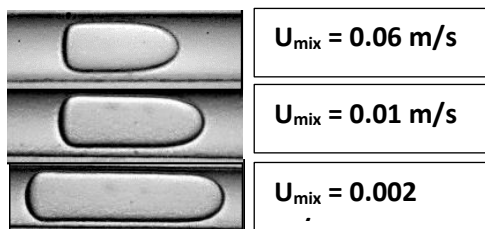
Fig. 8. Plug shape with increasing mixture velocity for 0.5 mm internal diameter channel. Ionic liquid is the continuous and aqueous the dispersed phase.

For the calculation of the plug interfacial area, it is assumed that the plugs have a capsule shape, with a cylindrical body and spherical ends, as illustrated in Fig. 9. A film with uniform thickness, δ, is then surrounding them. The surface area to volume ratio, α_p, was calculated as

follows, where SA_P is the surface area of the plug and V_{TU} is the total volume of the cell, which consists of a single plug and a single slug.
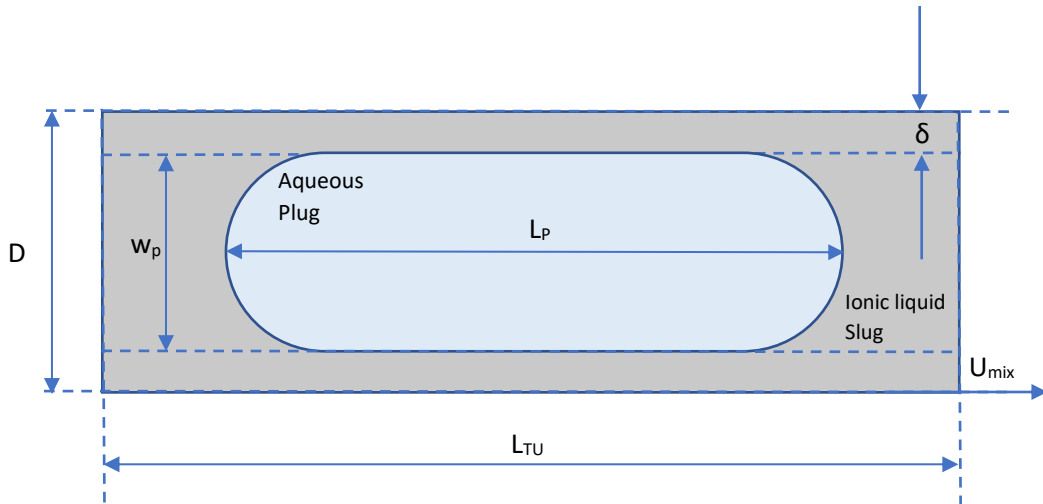
$$\alpha_p = \frac{SA_p}{V_{TU}} = \frac{\pi w_p L_p}{\pi \left(\frac{D}{2}\right)^2 L_{TU}} \tag{10}$$

The plug width, w_p is calculated from Eq. (11) from the average measured film thickness, δ.

$$w_p = D - 2\delta \tag{11}$$

For continuous phase volume fraction equal to 0.5, Eq. (10) becomes:

$$\alpha_p = \frac{6L_p}{3w_p L_p - w_p^2} \tag{12}$$

Fig. 9. Entire shell showing a single aqueous plug and the surrounding ionic liquid slug assuming equal ionic liquid to aqueous phase volume fraction.

The experimental specific interfacial areas calculated are approximately 4600, 2400 and 1300 m^2/m^3 for the 0.5, 1- and 2-mm internal diameter channels respectively, for the 0.01 m/s mixture velocity. The calculated interfacial areas with increasing mixture velocity are illustrated in Fig. 9 with a standard deviation of 3% (calculated from the standard deviation of the plug length measured from consecutive images). The thin film of the continuous phase surrounding the aqueous plugs means that the entire surface area of the plug is available for mass transfer. Although the chemical composition along the channel changes when extraction is occurring the concentrations are of 10^{-3} mol/L magnitude and the changes in the plug length, film thickness and consequently overall interfacial area are negligible.

Many different correlations have been proposed in the literature for calculating the film thickness [52]–[58] and the plug length using dimensionless numbers [16], [32], [59], [60]. From the available correlations for plug length, the correlation (Eq. (13)) by Tsaoulidis et. al, for the same system as the one used here, agreed well with the experimental data with an overestimation of ~ 8.3 % [32].

$$\frac{L_P}{d} = 2.2882 * Ca_{mix}^{0.2728} * Re_{mix}^{0.4617} * Re_c^{-0.9634} \tag{13}$$

The dimensionless Reynolds numbers in Eq. (13) are calculated separately for the mixture and the continuous ionic liquid phase, respectively.

$$Re_{mix} = \frac{\rho_c d u_{mix}}{\mu_c} \tag{14}$$

$$Re_c = \frac{\rho_c d u_c}{\mu_c} \tag{15}$$

Similarly, the correlation in Eq. (16) underestimated the film thickness by only ~ 6.5 % [32].

$$\frac{\delta}{d} = 0.329 Ca^{0.6409} Re^{0.1067} \tag{16}$$

Using Eq. (16) and Eq. (13) into Eq. (12), estimates of the interfacial area can be obtained which are shown against the ones calculated from the experimental plug length and film thickness in Fig. 10. As can be seen, the agreement is good with an average error of < 2% for $0.02 < Ca < 0.2$. The correlations for plug length and film thickness can therefore, be reliably used to estimate the interfacial area when experimental data are not available.

The range of interfacial areas obtained agreed with the values reported in the literature for two-phase liquid flows in small channels [32], [53], [61], [62]. Interfacial areas for liquid-liquid contactors such as packed and pulsed columns are about 250 m^2m^{-3} while the maximum reported for mixer-settlers is approximately 1000 m^2m^{-3} [63]–[65]. In this equipment a mean drop diameter is commonly used to predict the interfacial area, resulting in large standard deviations because of the wide drop size distributions. In contrast, the small channels offer not only larger specific interfacial areas compared to traditional equipment, but also more accurate estimates due to the low standard deviations of the plug lengths.
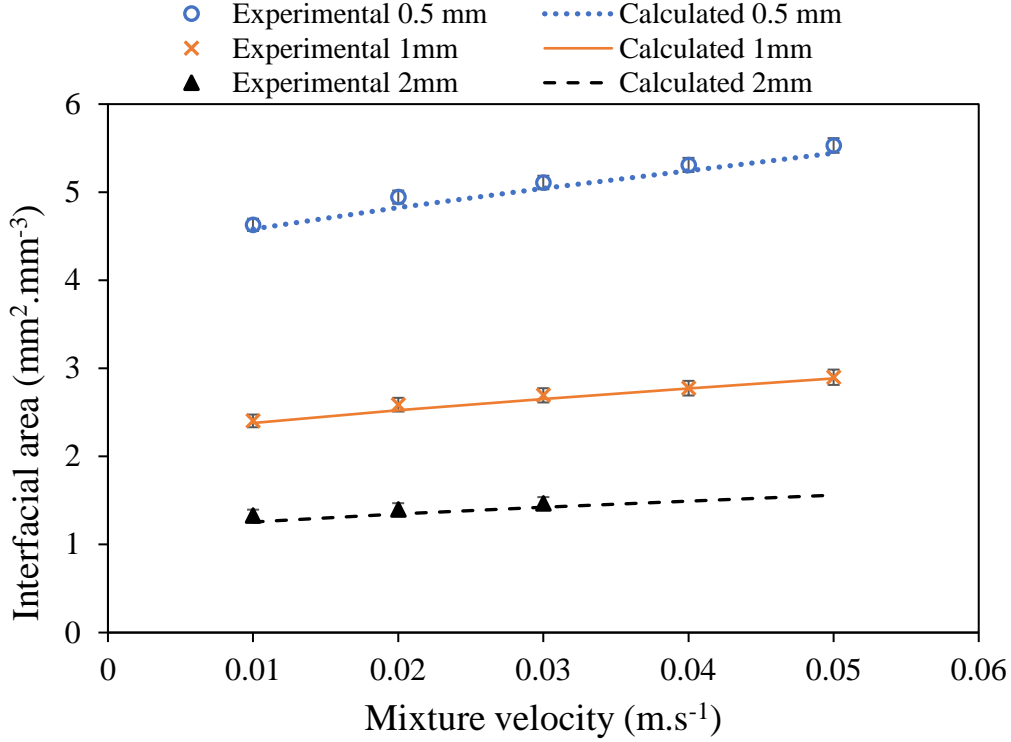
Fig. 10. Calculated interfacial area using dimensionless number for 0.5, 1 and 2 mm internal diameter channel versus experimental interfacial area acquired from image processing of plug length and film thickness.

6. Extraction in the small channels

Equal volumetric flow rates of the ionic liquid and aqueous phases were used for all the amino acid continuous extraction experiments. To characterise the mass transfer in the small channels, the percentage extraction (P%), the extraction efficiency (E%) compared to the equilibrium value and the overall volumetric mass transfer coefficients ($K_L\alpha$) were calculated using Eq. (17), (18) and (19) respectively [61].

$$P\% = \frac{C_{aq,in} - C_{aq,fin}}{C_{aq,in}} * 100 \qquad (17)$$

$$E\% = \frac{C_{aq,in} - C_{aq,fin}}{C_{aq,eq^*} - C_{aq,fin}} * 100 \qquad (18)$$

$$K_L a = \frac{1}{\tau} \ln\left(\frac{C_{aq,eq^*} - C_{aq,in}}{C_{aq,eq^*} - C_{aq,fin}}\right) \qquad (19)$$

where $C_{aqeq}{}^*$ is the maximum extracted L-tryptophan concentration determined from the equilibrium extractions. The residence time of the plugs in the channel, ($\tau = V_{ch}/ Q_{tot}$) was

19

determined as a function of the channel volume, V_{ch} (m^3) over the volumetric flow rate, Q_{mix} (m^{3}s^{-1}).

From the specific interfacial area, the mass transfer coefficient (K_L) for the small channel two-phase extraction system can be calculated using Eq. (20).

$$K_L = \frac{1}{a\,\tau} \ln\left(\frac{C_{aq,eq^*} - C_{aq,in}}{C_{aq,eq^*} - C_{aq,fin}}\right) \tag{20}$$

Following the equilibrium experiments the amino acid (0.0005 mol. L^{-1}) and the crown ether (0.002mol.L^{-1}) concentrations where kept constant for all flow experiments in the small channel system. These concentrations were chosen because high extraction efficiency was reported for low residence times during the equilibrium experiments. Channel lengths of 10 - 75 cm and appropriate mixture velocities were chosen, resulting in residence times of less than 30 seconds. These residence times were selected so that the extractions were not complete, and the effect of the individual parameters could be determined. The batch experiments showed that equilibrium could be reached quickly (less than 5 min). In addition, if 100% extraction were achieved within the channels, then the effects of residence time and hydrodynamics could not have been evaluated accordingly.

6.1 Effect of channel diameter on extraction efficiency

Fig. 10 illustrates the percentage extraction and extraction efficiency for the 0.5mm, 1mm and 2mm channels with increasing mixture velocity (0.01m/s-0.05m/s). In the 2mm channel extractions were not studied for mixture velocities > 0.04 m/s as the flow was on the boundary between the plug and the intermittent regime. Furthermore, in the flow separator at these high throughputs breakthrough of the aqueous phase into the IL phase happened and the samples could not be used for accurate concentration measurements. As can be seen from Fig. 10, with increasing mixture velocity, for all three channels, the percentage extraction and the extraction efficiency both decreased by approximately 10%. As the channel length was constant, at all experiments with increasing mixture velocity from 0.01 m/s to 0.05 m/s, the residence time decreased from 15 s to 3 s, while the interfacial area increased by approximately 20% (see Fig. 9). Both these two parameters affected mass transfer but in the opposite way. To isolate their effects on the extraction, the interfacial area and the residence time were studied separately, as described below in sections 6.2 and 6.3, respectively.

The results also show the large effect of the channel diameter on the extraction. As can be seen from Fig. 11 when the channel diameter decreases from 2 mm to 1 mm the extraction of L-

tryptophan increases by approximately 5% for all mixture velocities, while when it decreases from 1mm to 0.5 mm %E increases further by approximately 20%. An average 30% increase in the interfacial area was observed (see Fig. 10), when comparing the 2 mm channel to the 1 mm channel, and by approximately 48 % from the 1 mm to the 0.5 mm diameter channel.
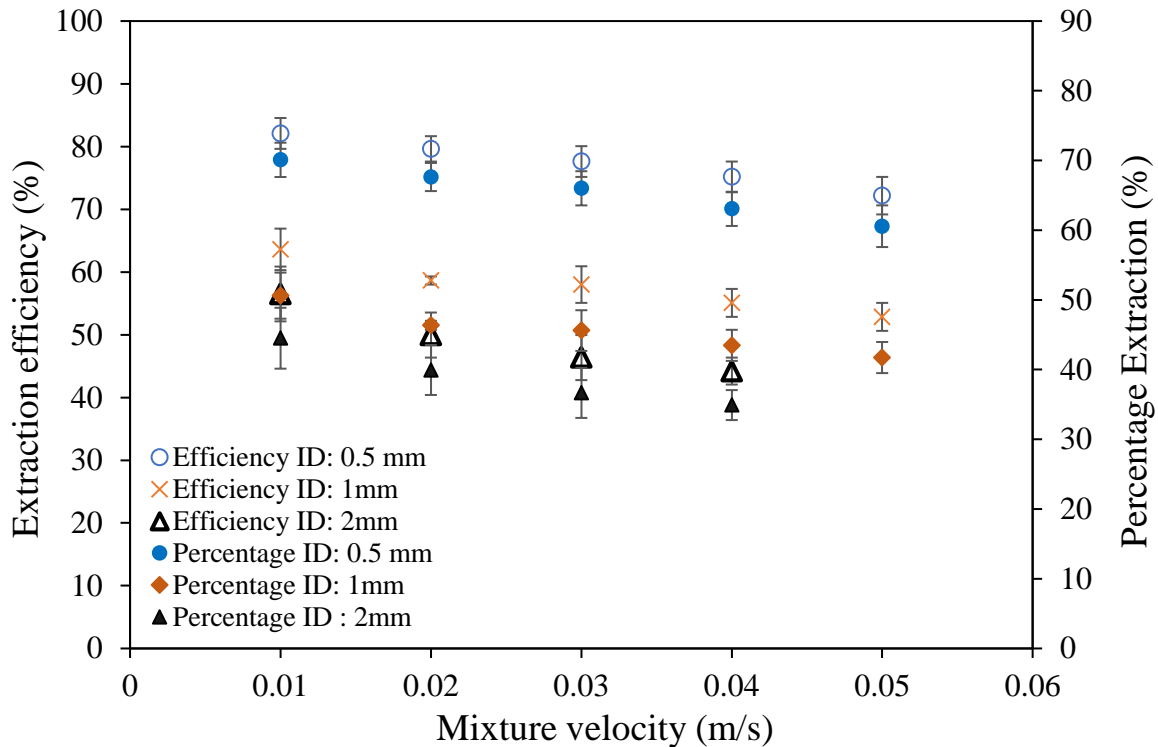
Fig. 11. Effect of channel dimeter with constant channel length (15 cm) on the extraction efficiency and percentage extraction of L-tryptophan in ionic liquid [C4mim][NTf2] in small channels.
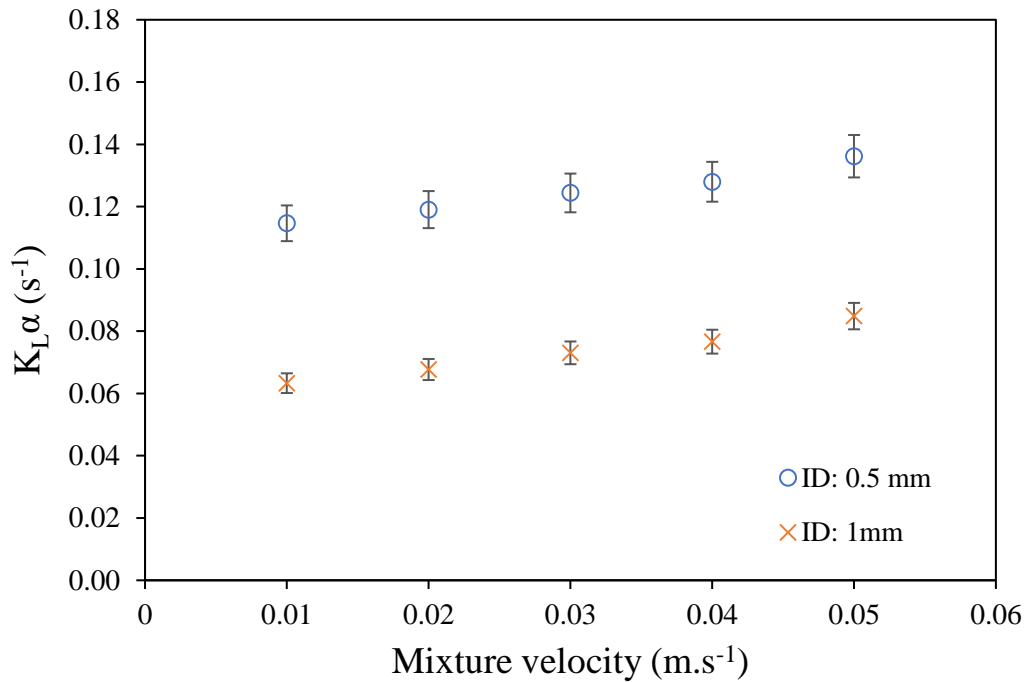
6.2 Effect of mixture velocity on extraction efficiency

To isolate the effect of the mixture velocity on the mass transfer, in the following results shown in Fig. 12, the residence time was kept constant and equal to 15 seconds by changing the channel length. For mixture velocities from 0.01 to 0.05 m/s the channel length increased from 15 to 75 cm. For the 0.5 mm channel, when the mixture velocity increased from 0.01m/s to 0.05 m/s the extraction efficiency, E%, increased by 6% while the interfacial area increased by approximately 19% (see Fig.10). With increasing mixture velocity, the internal circulation within each aqueous plug increases, enhancing the mass transfer [52]. Similarly, for the same increase in mixture velocity in the 1mm channel there was approximately an 8% increase in the extraction efficiency and a 20% increase in the interfacial area available for mass transfer.
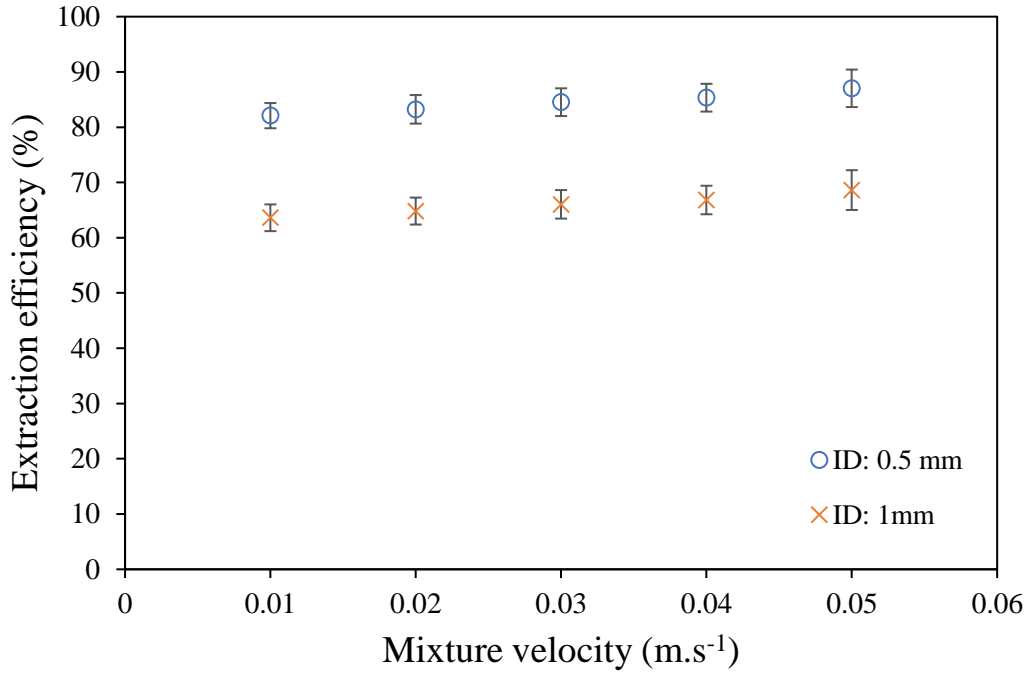
Fig. 12. Isolated effect of extraction efficiency on the extraction efficiency of L-tryptophan with increasing mixture velocity (0.01 to 0.05 m/s), increasing channel length (15-75 cm) and constant residence time (15s).

For the same experimental conditions, the overall volumetric mass transfer coefficient was also determined using Eq (19). There is an increase in the $K_L\alpha$ with increasing mixture velocity as shown in Fig. 13 for both the 0.5 and 1 mm channels. Literature $K_L\alpha$ values range from 0.11-0.13 and 0.06-0.08 s^{-1} for the 0.5 and the 1mm channels respectively for a residence time of 15 s. From the estimates of the interfacial area, α ($m^2.m^{-3}$) the K_L ($m.s^{-1}$) of the system could be determined with Eq (20). The K_L was found to be approximately equal to 2.4 x10^{-5} $m.s^{-1}$ ± 4% for the 0.5 mm channel and to 2.6 x10^{-5} $m.s^{-1}$ ± 8% for the 1mm channel and in the same order of magnitude as conventional equipment [53]. This indicates that the interfacial area in small channel extractors is mainly responsible for the large overall mass transfer coefficients, compared to conventional extractors

Fig. 13. Overall mass transfer coefficient values for 0.5 and 1mm internal diameter channels with increasing mixture velocity (0.01-0.05 m/s) and constant residence time (15s).

6.3 Effect of residence time on extraction efficiency

To investigate and isolate the effect of residence time on mass transfer, the mixture velocity was kept constant at 0.01m/s while the channel length varied from 15 -30 cm. Lower residence times than those required to reach equilibrium were selected to be able to investigate the effects of different parameters on extraction. As illustrated in Fig. 14, the extraction efficiencies of the amino acid were larger in the 0.5 mm channel compared to the 1 mm one. In the 0.5 mm channel, the extraction efficiency is 20% greater than in the 1mm channel at low residence times and approximately 15% at high residence times. The interfacial area at each channel size was constant as the mixture velocity did not change (1300 $m^2.m^{-3}$ for the 2 mm and 4600 $m^2.m^{-3}$ for the 0.5 mm channel) and was assumed to have a negligible effect on the extraction efficiency since the mixture velocity was the same for all experiments. The extraction efficiency increases with residence time in both channels, but this increase is larger in the 1 mm channel (23%) compared to the 0.5 mm channel (18%) when the residence time increases from 15 to 30 seconds. This is probably because with increasing residence time in the small channel the extraction efficiency approaches the maximum value and thus the concentration difference that drives the mass transfer is reduced. For comparison, the required residence times for extraction in mixers are 1-10 min and additional settling (separation) times [66].
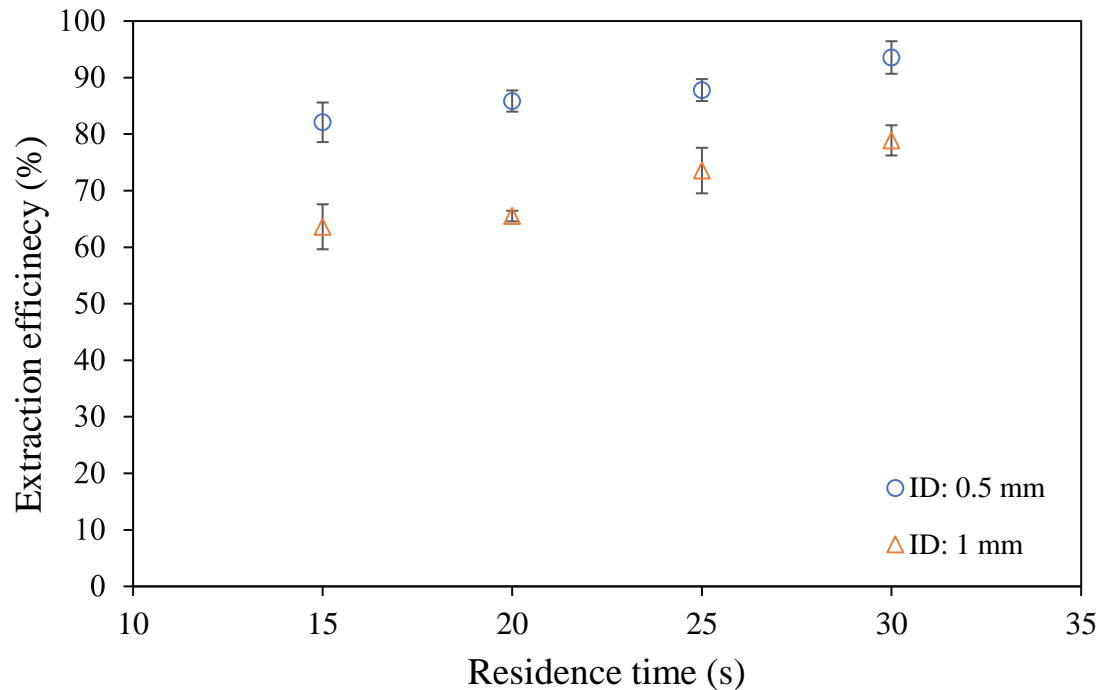
Fig. 14. Effect of extraction of amino acid with increasing residence time for 0.5 and 1mm channels. Residence time varied from 15 to 30 seconds.

As can be seen from Fig. 15 the overall mass transfer coefficients where larger in the smaller channel and decreased with increasing residence time initially before reaching a plateau. The results suggest that the mass transfer coefficient is largest at the beginning of the channel close to the inlet, where there is intense mixing when the two phases meet and there is change of the flow direction. Further downstream the channel, where the plug flow is fully established, the mass transfer coefficient acquired an almost constant value. If the effect of the inlet is excluded, the overall mass transfer coefficient is about 0.09 s^{-1} and 0.05 s^{-1} for the 0.5 and 1 mm channels respectively. Similar observations have been reported previously in the literature [32], [53]. As the channel length is increased the effect of the inlet on the overall volumetric mass transfer coefficient decreases.

To select the optimum residence time, the extraction needs to be considered within the whole process flowsheet (see for example [67], [68]). The results reported here on mass transfer coefficients can be used to study and optimize such process flowsheets.
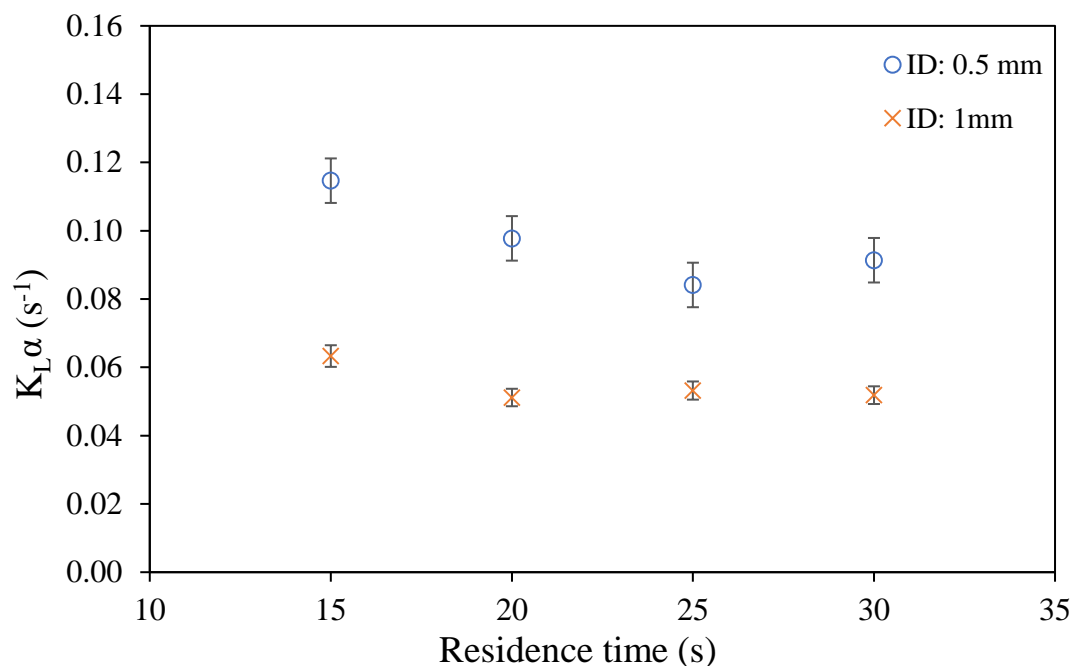
Fig. 15. Overall volumetric mass transfer coefficient with increasing residence time and constant mixture velocity (0.01 m/s) for 0.5- and 1-mm channel.

7. Conclusions

In this work, the continuous flow extraction of the amino acid L-tryptophan from aqueous solutions in small channels with diameters 0.5-2 mm, using ionic liquids was investigated. A new extraction system was identified using the hydrophobic ionic liquid 1-Butyl-3-methylimidazolium Bis (trifluoromethanesulfonyl)imide, [C4mim][Tf$_2$N] and crown ether Dicyclohexano-18-crown-6 as an extractant. From equilibrium experiments an extraction mechanism was proposed involving the ammonium centre of the amino acid forming hydrogen bonds with the 18-crown-6 part of the crown ether with a 1:1 ratio of amino acid to extractant (Fig. 4).

Flow pattern maps were developed for all channel diameters, which indicated the conditions under which plug flow is established. Based on these, the continuous extraction experiments in the small channels were carried out for mixture velocities 0.01-0.06 m/s and equal ionic liquid and aqueous phase volume fractions, ensuring plug flow regime. The interfacial areas were calculated from images and revealed to greatly affect the extraction efficiency; a 70% increase in the specific interfacial area available for mass transfer was observed when the internal channel diameter decreased from 2 mm to 0.5 mm (Fig. 10). The amino acid concentration was kept constant at 0.005 mol.L^{-1} for all extraction experiments performed in the small channels.

For the 15 cm channel length and 0.01m/s mixture velocity the extraction efficiencies reported reached 57 % in the 2mm channel and increased to 82% in the 0.5 mm channel. In just 30s the maximum efficiency achieved in the 0.5 mm and 1 mm channels reached 94% and 79% respectively, as opposed to traditional apparatus that require several minutes to reach equilibrium (see Fig. 14). The overall mass transfer coefficients, $K_L\alpha$, were in all cases studied in the range of 0.1 s^{-1} (see Fig.15), which is 1-2 orders of magnitude greater than in equipment such as mixer-settlers and pulsed columns. This was attributed mainly to the interfacial area, α, available for mass transfer which reached up to 5500 m^2 m^{-3} in the 0.5 mm channel.

The results demonstrate that the novel combination of small channels and ionic liquid solvents results in large extraction efficiencies of amino acids within short residence times. For the scale up of the small channel contactors, a compromise is needed on the channel size that ensures enhanced mass transfer rates and large throughputs. The approach can be used for the separation of other amino acids or more complex biomolecules such as peptides, enzymes and proteins. In the future, we plan to combine the extraction step with the ionic liquid regeneration in back extraction (e.g. [28]). We will also investigate the increase in throughput by considering scale our approaches where multiple channels are used in parallel.

Acknowledgments

8. References

[1]   J. Rydberg, Ed., *Solvent Extraction Principles and Practice, Revised and Expanded*. CRC Press, 2004.

[2]   T. Itoh and Y.-M. Koo, Eds., *Application of Ionic Liquids in Biotechnology*, vol. 168. Cham: Springer International Publishing, 2019.

[3]   S. Behme, *Manufacturing of Pharmaceutical Proteins*. Weinheim, Germany: Wiley-VCH Verlag GmbH & Co. KGaA, 2015.

[4]   C. Tonhauser, A. Natalello, H. Löwe, and H. Frey, "Microflow Technology in Polymer Synthesis," *Macromolecules*, vol. 45, no. 24, Dec. 2012, doi: 10.1021/ma301671x.

[5]   D. Ciceri, J. M. Perera, and G. W. Stevens, "The use of microfluidic devices in solvent extraction," *J. Chem. Technol. Biotechnol.*, vol. 89, no. 6, Jun. 2014, doi: 10.1002/jctb.4318.

[6] K. Wang and G. Luo, "Microflow extraction: A review of recent development," *Chem. Eng. Sci.*, vol. 169, Sep. 2017, doi: 10.1016/j.ces.2016.10.025.

[7] A. Stankiewicz and J. A. Moulijn, "Process Intensification," *Ind. Eng. Chem. Res.*, vol. 41, no. 8, Apr. 2002, doi: 10.1021/ie011025p.

[8] M. Sattari-Najafabadi, M. Nasr Esfahany, Z. Wu, and B. Sunden, "Mass transfer between phases in microchannels: A review," *Chem. Eng. Process. - Process Intensif.*, vol. 127, May 2018, doi: 10.1016/j.cep.2018.03.012.

[9] C. Xu and T. Xie, "Review of Microfluidic Liquid–Liquid Extractors," *Ind. Eng. Chem. Res.*, vol. 56, no. 27, Jul. 2017, doi: 10.1021/acs.iecr.7b01712.

[10] P. Angeli, E. G. Ortega, D. Tsaoulidis, and M. Earle, "Intensified liquid-liquid extraction technologies in small channels: A review," *Johnson Matthey Technology Review*, vol. 63, no. 4. Johnson Matthey Public Limited Company, pp. 299–310, Oct. 01, 2019, doi: 10.1595/205651319X15669171624235.

[11] K. W. Oh, "Microfluidic Devices for Biomedical Applications: Biomedical Microfluidic Devices 2019," *Micromachines*, vol. 11, no. 4, Apr. 2020, doi: 10.3390/mi11040370.

[12] J. Kim *et al.*, "Applications, techniques, and microfluidic interfacing for nanoscale biosensing," *Microfluid. Nanofluidics*, vol. 7, no. 2, Aug. 2009, doi: 10.1007/s10404-009-0431-8.

[13] F. A. Vicente, I. Plazl, S. P. M. Ventura, and P. Žnidaršič-Plazl, "Separation and purification of biomacromolecules based on microfluidics," *Green Chem.*, vol. 22, no. 14, 2020, doi: 10.1039/C9GC04362D.

[14] A. Mitic and K. V. Gernaey, "Process Intensification Tools in the Small-Scale Pharmaceutical Manufacturing of Small Molecules," *Chem. Eng. Technol.*, vol. 38, no. 10, Oct. 2015, doi: 10.1002/ceat.201400765.

[15] J. Jovanović, W. Zhou, E. V. Rebrov, T. A. Nijhuis, V. Hessel, and J. C. Schouten, "Liquid–liquid slug flow: Hydrodynamics and pressure drop," *Chem. Eng. Sci.*, vol. 66, no. 1, Jan. 2011, doi: 10.1016/j.ces.2010.09.040.

[16] M. N. Kashid and D. W. Agar, "Hydrodynamics of liquid–liquid slug flow capillary microreactor: Flow regimes, slug size and pressure drop," *Chem. Eng. J.*, vol. 131, no.

1–3, Jul. 2007, doi: 10.1016/j.cej.2006.11.020.

[17] D. Tsaoulidis, V. Dore, P. Angeli, N. V. Plechkova, and K. R. Seddon, "Flow patterns and pressure drop of ionic liquid-water two-phase flows in microchannels," *Int. J. Multiph. Flow*, vol. 54, pp. 1–10, Sep. 2013, doi: 10.1016/j.ijmultiphaseflow.2013.02.002.

[18] N. Assmann, A. Ładosz, and P. Rudolf von Rohr, "Continuous Micro Liquid-Liquid Extraction," *Chem. Eng. Technol.*, vol. 36, no. 6, Jun. 2013, doi: 10.1002/ceat.201200557.

[19] Y. Mahdi, K. Daoud, and L. Tadrist, "Two-phase flow patterns and size distribution of droplets in a microfluidic T-junction: Experimental observations in the squeezing regime," *Comptes Rendus Mécanique*, vol. 345, no. 4, Apr. 2017, doi: 10.1016/j.crme.2017.02.001.

[20] Z. Cao, Z. Wu, and B. Sundén, "Dimensionless analysis on liquid-liquid flow patterns and scaling law on slug hydrodynamics in cross-junction microchannels," *Chem. Eng. J.*, vol. 344, Jul. 2018, doi: 10.1016/j.cej.2018.03.119.

[21] M. Darekar, K. K. Singh, S. Mukhopadhyay, and K. T. Shenoy, "Liquid–Liquid Two-Phase Flow Patterns in Y-Junction Microchannels," *Ind. Eng. Chem. Res.*, vol. 56, no. 42, Oct. 2017, doi: 10.1021/acs.iecr.7b03164.

[22] Q. Zhang, H. Liu, S. Zhao, C. Yao, and G. Chen, "Hydrodynamics and mass transfer characteristics of liquid–liquid slug flow in microchannels: The effects of temperature, fluid properties and channel size," *Chem. Eng. J.*, vol. 358, Feb. 2019, doi: 10.1016/j.cej.2018.10.056.

[23] M. N. Kashid, A. Renken, and L. Kiwi-Minsker, "Gas–liquid and liquid–liquid mass transfer in microstructured reactors," *Chem. Eng. Sci.*, vol. 66, no. 17, Sep. 2011, doi: 10.1016/j.ces.2011.05.015.

[24] R. Seemann, M. Brinkmann, T. Pfohl, and S. Herminghaus, "Droplet based microfluidics," *Reports Prog. Phys.*, vol. 75, no. 1, Jan. 2012, doi: 10.1088/0034-4885/75/1/016601.

[25] J. Qian, X. Li, Z. Wu, Z. Jin, and B. Sunden, "A comprehensive review on liquid–liquid two-phase flow in microchannel: flow pattern and mass transfer," *Microfluid.*

Nanofluidics, vol. 23, no. 10, Oct. 2019, doi: 10.1007/s10404-019-2280-4.

[26]   Y. Kohno and H. Ohno, "Ionic liquid/water mixtures: from hostility to conciliation," *Chem. Commun.*, vol. 48, no. 57, 2012, doi: 10.1039/c2cc31638b.

[27]   L. I. N. Tomé *et al.*, "On the Interactions between Amino Acids and Ionic Liquids in Aqueous Media," *J. Phys. Chem. B*, vol. 113, no. 42, Oct. 2009, doi: 10.1021/jp906481m.

[28]   S. V. Smirnova, I. I. Torocheshnikova, A. A. Formanovsky, and I. V. Pletnev, "Solvent extraction of amino acids into a room temperature ionic liquid with dicyclohexano-18-crown-6," *Anal. Bioanal. Chem.*, vol. 378, no. 5, Mar. 2004, doi: 10.1007/s00216-003-2398-8.

[29]   C. M. S. S. Neves, S. P. M. Ventura, M. G. Freire, I. M. Marrucho, and J. A. P. Coutinho, "Evaluation of Cation Influence on the Formation and Extraction Capability of Ionic-Liquid-Based Aqueous Biphasic Systems," *J. Phys. Chem. B*, vol. 113, no. 15, Apr. 2009, doi: 10.1021/jp900293v.

[30]   H. Vallette, L. Ferron, G. Coquerel, A.-C. Gaumont, and J.-C. Plaquevent, "Peptide synthesis in room temperature ionic liquids," *Tetrahedron Lett.*, vol. 45, no. 8, Feb. 2004, doi: 10.1016/j.tetlet.2003.12.124.

[31]   S. Carda–Broch, A. Berthod, and D. W. Armstrong, "Solvent properties of the 1-butyl-3-methylimidazolium hexafluorophosphate ionic liquid," *Anal. Bioanal. Chem.*, vol. 375, no. 2, Jan. 2003, doi: 10.1007/s00216-002-1684-1.

[32]   D. Tsaoulidis and P. Angeli, "Effect of channel size on mass transfer during liquid–liquid plug flow in small scale extractors," *Chem. Eng. J.*, vol. 262, Feb. 2015, doi: 10.1016/j.cej.2014.10.012.

[33]   C. F. Poole and S. K. Poole, "Extraction of organic compounds with room temperature ionic liquids," *J. Chromatogr. A*, vol. 1217, no. 16, Apr. 2010, doi: 10.1016/j.chroma.2009.09.011.

[34]   N. V. Plechkova and K. R. Seddon, "Applications of ionic liquids in the chemical industry," *Chem. Soc. Rev.*, vol. 37, no. 1, 2008, doi: 10.1039/B006677J.

[35]   S. K. Singh and A. W. Savoy, "Ionic liquids synthesis and applications: An overview," *J. Mol. Liq.*, vol. 297, Jan. 2020, doi: 10.1016/j.molliq.2019.112038.

[36] S. P. M. Ventura, F. A. e Silva, M. V. Quental, D. Mondal, M. G. Freire, and J. A. P. Coutinho, "Ionic-Liquid-Mediated Extraction and Separation Processes for Bioactive Compounds: Past, Present, and Future Trends," *Chem. Rev.*, vol. 117, no. 10, May 2017, doi: 10.1021/acs.chemrev.6b00550.

[37] L. Huaxi *et al.*, "Liquid–liquid extraction process of amino acids by a new amide-based functionalized ionic liquid," *Green Chem.*, vol. 14, no. 6, pp. 1721–1727, Jun. 2012, doi: 10.1039/c2gc16560k.

[38] K. Shimojo, K. Nakashima, N. Kamiya, and M. Goto, "Crown ether-mediated extraction and functional conversion of cytochrome C in ionic liquids.," *Biomacromolecules*, vol. 7, no. 1, Jan. 2006, doi: 10.1021/bm050847t.

[39] J. Wang, Y. Pei, Y. Zhao, and Z. Hu, "Recovery of amino acids by imidazolium based ionic liquids from aqueous media," *Green Chem.*, vol. 7, no. 4, 2005, doi: 10.1039/b415842c.

[40] L. I. N. Tomé, V. R. Catambas, A. R. R. Teles, M. G. Freire, I. M. Marrucho, and J. A. P. Coutinho, "Tryptophan extraction using hydrophobic ionic liquids," *Sep. Purif. Technol.*, vol. 72, no. 2, Apr. 2010, doi: 10.1016/j.seppur.2010.02.002.

[41] A. Seduraman, P. Wu, and M. Klähn, "Extraction of Tryptophan with Ionic Liquids Studied with Molecular Dynamics Simulations," *J. Phys. Chem. B*, vol. 116, no. 1, Jan. 2012, doi: 10.1021/jp206748z.

[42] G. Absalan, M. Akhond, and L. Sheikhian, "Partitioning of acidic, basic and neutral amino acids into imidazolium-based ionic liquids," *Amino Acids*, vol. 39, no. 1, Jun. 2010, doi: 10.1007/s00726-009-0391-z.

[43] S. Dreyer and U. Kragl, "Ionic liquids for aqueous two-phase extraction and stabilization of enzymes," *Biotechnol. Bioeng.*, vol. 99, no. 6, Apr. 2008, doi: 10.1002/bit.21720.

[44] T. Vasantha, A. Kumar, P. Attri, P. Venkatesu, and R. S. Devi, "The Solubility and Stability of Amino Acids in Biocompatible Ionic Liquids," *Protein Pept. Lett.*, vol. 21, no. 1, Dec. 2013, doi: 10.2174/09298665113209990071.

[45] A. S. Paluch, C. A. Vitter, J. K. Shah, and E. J. Maginn, "A comparison of the solvation thermodynamics of amino acid analogues in water, 1-octanol and 1-n-alkyl-

3-methylimidazolium bis(trifluoromethylsulfonyl)imide ionic liquids by molecular simulation.," *J. Chem. Phys.*, vol. 137, no. 18, Nov. 2012, doi: 10.1063/1.4765097.

[46] M. G. Freire, C. M. S. S. Neves, I. M. Marrucho, J. A. P. Coutinho, and A. M. Fernandes, "Hydrolysis of Tetrafluoroborate and Hexafluorophosphate Counter Ions in Imidazolium-Based Ionic Liquids," *J. Phys. Chem. A*, vol. 114, no. 11, Mar. 2010, doi: 10.1021/jp903292n.

[47] J. Al-Mustafa, S. Hamzah, and D. Marji, "Thermodynamics of Amino Acid Methyl Ester Hydrochlorides," *J. Solution Chem.*, vol. 30, no. 8, 2001, doi: 10.1023/A:1011953211179.

[48] N. E. Kuz'mina *et al.*, "Complex formation of crown ethers with α-amino acids: Estimation by NMR spectroscopy," *Russ. J. Org. Chem.*, vol. 49, no. 9, Sep. 2013, doi: 10.1134/S1070428013090261.

[49] T. R. Usacheva and V. A. Sharnin, "A thermodynamic study of reactions of amino acids with crown ethers in nonaqueous media as examples of guest—host molecular complex formation," *Russ. Chem. Bull.*, vol. 64, no. 11, Nov. 2015, doi: 10.1007/s11172-015-1189-7.

[50] M. Koźbiał and J. Poznański, "Experimental evidence of chiral crown ether complexation with aromatic amino acids," *J. Phys. Org. Chem.*, vol. 20, no. 7, Jul. 2007, doi: 10.1002/poc.1189.

[51] P. Angeli and A. Gavriilidis, "Hydrodynamics of Taylor flow in small channels: A Review," *Proc. Inst. Mech. Eng. Part C J. Mech. Eng. Sci.*, vol. 222, no. 5, May 2008, doi: 10.1243/09544062JMES776.

[52] V. Dore, D. Tsaoulidis, and P. Angeli, "Mixing patterns in water plugs during water/ionic liquid segmented flow in microchannels," *Chem. Eng. Sci.*, vol. 80, Oct. 2012, doi: 10.1016/j.ces.2012.06.030.

[53] E. Garciadiego-Ortega, D. Tsaoulidis, M. Pineda, E. S. Fraga, and P. Angeli, "Hydrodynamics and mass transfer in segmented flow small channel contactors for uranium extraction," *Chem. Eng. Process. - Process Intensif.*, vol. 153, Jul. 2020, doi: 10.1016/j.cep.2020.107921.

[54] F. P. Bretherton, "The motion of long bubbles in tubes," *J. Fluid Mech.*, vol. 10, no.

02, Mar. 1961, doi: 10.1017/S0022112061000160.

[55]   P. Aussillous and D. Quéré, "Quick deposition of a fluid on the wall of a tube," *Phys. Fluids*, vol. 12, no. 10, 2000, doi: 10.1063/1.1289396.

[56]   S. Irandoust and B. Andersson, "Liquid film in Taylor flow through a capillary," *Ind. Eng. Chem. Res.*, vol. 28, no. 11, Nov. 1989, doi: 10.1021/ie00095a018.

[57]   Y. Han and N. Shikazono, "Measurement of the liquid film thickness in micro tube slug flow," *Int. J. Heat Fluid Flow*, vol. 30, no. 5, Oct. 2009, doi: 10.1016/j.ijheatfluidflow.2009.02.019.

[58]   M. Mac Giolla Eain, V. Egan, and J. Punch, "Film thickness measurements in liquid–liquid slug flow regimes," *Int. J. Heat Fluid Flow*, vol. 44, Dec. 2013, doi: 10.1016/j.ijheatfluidflow.2013.08.009.

[59]   J. H. Xu, S. W. Li, J. Tan, and G. S. Luo, "Correlations of droplet formation in T-junction microfluidic devices: From squeezing to dripping," *Microfluid. Nanofluidics*, vol. 5, no. 6, pp. 711–717, 2008, doi: 10.1007/s10404-008-0306-4.

[60]   Q. Li and P. Angeli, "Experimental and numerical hydrodynamic studies of ionic liquid-aqueous plug flow in small channels," *Chem. Eng. J.*, vol. 328, Nov. 2017, doi: 10.1016/j.cej.2017.07.037.

[61]   M. N. Kashid, Y. M. Harshe, and D. W. Agar, "Liquid−Liquid Slug Flow in a Capillary: An Alternative to Suspended Drop or Film Contactors," *Ind. Eng. Chem. Res.*, vol. 46, no. 25, Dec. 2007, doi: 10.1021/ie070077x.

[62]   M. Sattari-Najafabadi and M. N. Nasr Esfahany, "Intensification of liquid-liquid mass transfer in a circular microchannel in the presence of sodium dodecyl sulfate," *Chem. Eng. Process. Process Intensif.*, vol. 117, Jul. 2017, doi: 10.1016/j.cep.2017.03.011.

[63]   R. P. Verma and M. M. Sharma, "Mass transfer in packed liquid—liquid extraction columns," *Chem. Eng. Sci.*, vol. 30, no. 3, Mar. 1975, doi: 10.1016/0009-2509(75)80078-9.

[64]   M. Torab-Mostaedi, A. Ghaemi, and M. Asadollahzadeh, "Prediction of mass transfer coefficients in a pulsed disc and doughnut extraction column," *Can. J. Chem. Eng.*, vol. 90, no. 6, Dec. 2012, doi: 10.1002/cjce.20649.

[65] M. M. Sharma and L. K. Doraiswamy, *Heterogeneous reactions: Analysis, examples, and reactor design.*, vol. 31. 1985.

[66] G. A. Pinto, F. O. Durão, A. M. A. Fiúza, M. M. B. L. Guimarães, and C. M. N. Madureira, "Design optimisation study of solvent extraction: chemical reaction, mass transfer and mixer–settler hydrodynamics," *Hydrometallurgy*, vol. 74, no. 1–2, Aug. 2004, doi: 10.1016/j.hydromet.2004.02.002.

[67] D. Bascone, P. Angeli, and E. S. Fraga, "A modelling approach for the comparison between intensified extraction in small channels and conventional solvent extraction technologies," *Chem. Eng. Sci.*, vol. 203, pp. 201–211, Aug. 2019, doi: 10.1016/j.ces.2019.03.074.

[68] D. Bascone, P. Angeli, and E. S. Fraga, "Process intensification applied to spent nuclear fuel reprocessing: An alternative flowsheet using small channels," *Chem. Eng. Process. - Process Intensif.*, vol. 143, p. 107618, Sep. 2019, doi: 10.1016/j.cep.2019.107618.